*Materials Transactions*, Vol. 48, No. 11 (2007) pp. 2923 to 2927


# Theory of Shear Banding in Metallic Glasses and Molecular Dynamics Calculations

Futoshi Shimizu[1,2], Shigenobu Ogata[3] and Ju Li[2,*]

[1] *Center for Computational Science & e-Systems, Japan Atomic Energy Agency, Tokyo 110-0015, Japan*
[2] *Department of Materials Science and Engineering, Ohio State University, Columbus, OH 43210, USA*
[3] *Department of Mechanical Science and Bioengineering, Graduate School of Engineering Science, Osaka University, Osaka 560-8531, Japan*

The aged-rejuvenation-glue-liquid (ARGL) shear band model has been proposed for metallic glasses (Acta Mater. **54** (2006) 4293), based on small-scale molecular dynamics simulations up to 20,000 atoms and thermomechanical analysis. The model predicts the existence of a critical lengthscale ~10 nm, above which melting could occur in shear-alienated glass. Large-scale molecular dynamics simulations with up to 5 million atoms have directly verified this prediction. When the applied stress exceeds the glue traction (computed separately before in a shear cohesive zone, or an amorphous-amorphous "generalized stacking fault energy" calculation), we indeed observe maturation of the shear band embryo into bona fide shear crack, accompanied by melting. In contrast, when the applied stress is below the glue traction, the shear band embryo does not propagate, becomes diffuse, and eventually dies. Thus this all-important quantity, the glue traction which is a property of shear-alienated glass, controls the macroscopic yield point of well-aged glass. We further suggest that the disruption of chemical short-range order ("chemical softening") governs the glue traction microscopically. Catastrophic thermal softening occurs only after chemical alienation and softening in our simulation, after the shear band embryo has already run a critical length. [doi:10.2320/matertrans.MJ200769]

(Received December 1, 2006; Accepted August 17, 2007; Published October 18, 2007)

***Keywords:*** *shear cohesive zone, chemical softening, incubation lengthscale, thermal softening*

## 1. Introduction

Bulk metallic glasses (BMGs) are new materials[1] with very high strength, low internal friction and good corrosion resistance. The uniaxial yield strain of most BMGs falls within a small range around $\epsilon_y \simeq 2\%$ at room temperature,[1,2] beyond which shear bands nucleate and propagate globally.[3,4] We have previously proposed the aged-rejuvenation-glue-liquid (ARGL) model of shear band in BMGs.[5] The model argues that the $\epsilon_y$ condition corresponds to embryonic shear band (ESB) propagation, not its nucleation. To propagate an embryonic shear band, the far-field shear stress $\tau_\infty \approx E\epsilon_y/2$ must exceed the quasi steady-state glue traction $\tau_{glue}$ of shear-alienated glass (shear cohesive zone) until the glass-transition temperature $T_g$ is approached internally due to frictional heating, at which point ESB matures as a runaway shear crack, since the trailing $T > T_g$ zone would have much lower viscosity than the shear cohesive zone and can be regarded as shear traction free. The magnitude of $\tau_{glue}$ is governed by competing alienation and recovery processes. Alienation is the disruption of short-range order (including chemical ordering[6]) due to fast localized shearing. Recovery is the counter-acting diffusionless downhill process that recovers part of that short-range order.

It was predicted that the alienation and recovery dynamics fall into the accessible timescale of ordinary molecular dynamics (MD) simulations. Thus MD calculations should be able to capture the dynamics of ESB and hence the $\epsilon_y$ value of BMGs. In our previous paper,[5] although we proposed the ARGL model based on small-scale atomistic simulations and theoretical analysis, we have not confirmed it directly using more realistic boundary condition and large-scale MD simulation. In this paper we present a brief outline of the ARGL model and the calculations of $\tau_{glue}$ by small-scale MD simulations of the shear cohesive zone ("generalized stacking fault energy"[5]), as well as large-scale MD simulations which directly verify the ARGL "march-to-melting" prediction, within a spatial-temporal domain of ~200 nm and ~1000 ps.

*Corresponding author, E-mail: li.562@osu.edu

## 2. Shear Band Model

A mature shear band (MSB) in BMG is proposed to be similar to a mode-II or III dynamical crack, driven by far-field shear stress $\tau_\infty$.[5] The tail of the band is liquid or near-liquid, due to friction-induced high temperature $T \sim T_g$ ($T_g$ is the glass transition temperature), and is essentially traction-free. The band tip is the rejuvenation zone, where the glass undergoes transition from well-aged to rejuvenated state,[7] under a locally very high shear stress $\tau > \tau_r$, where $\tau_r$ is the rejuvenation stress. $\tau_r$ is an intrinsic property of well-aged glass, but its value is not relevant to the $\epsilon_y$ value.[5] The intermediate region between the band tip and the liquid tail is the "glue" zone, similar to the cohesive zone in fracture mechanics[8] in the shear sense: its temperature is below $T_g$ and consists of shear-rejuvenated and subsequently shear-alienated glass. Alienation is a special form of rejuvenation[7] in the limit of intense localized shearing at extremely fast rates. Because of shearing, the original first-nearest-neighbor relations and chemical ordering[6] are severely disrupted at the atomic level in the glue zone. The traction this shear cohesive zone or glue zone ($T < T_g$) offers, $\tau_{glue}$, is the main resistance against shear band propagation. The shear cohesive law is the equivalent of generalized stacking fault energy in crystalline materials,[9] but for an amorphous-amorphous interface.[5]

We define the embryonic shear band (ESB) as a shear band embryo with long aspect ratio, but which has no liquid zone, since the internal temperature has not risen high enough yet. To propagate an ESB, the far-field shear stress $\tau_\infty \approx E\epsilon_y/2$ must exceed the quasi steady-state glue traction $\tau_{glue}$ of shear-alienated glass in the shear cohesive zone until the glass-transition temperature $T_g$ is approached internally due to frictional heating, at which point ESB matures as a runaway shear crack. At the ESB tip, the local shear stress is amplified as $\tau \propto (\tau_\infty - \tau_{\rm glue})\sqrt{a/w}$ according to the stress solution for an elliptical hole, where $a$ is the length of the ESB, and $w$ is its width as an approximant of the ESB tip curvature. This means that as long as the embryo has a large aspect ratio $a/w$, $\tau_{\rm r}$ can always be exceeded at the tip if $\tau_\infty > \tau_{\rm glue}$. We further assume there are plenty of pre-existing embryos in the BMG sample. But if $\tau_\infty < \tau_{\rm glue}$, even with plenty of embryos, they still cannot propagate.

When $\tau_\infty > \tau_{\rm glue}$, an embryo can run, but it cannot run to maturity if the size of the $\tau_\infty > \tau_{\rm glue}$ region is smaller than an incubation lengthscale $l_{\rm inc}$, estimated to be

$$l_{\rm inc} \sim \frac{\alpha c_v^2 (T_{\rm g} - T_{\rm env})^2}{\tau_{\rm glue}^2 c_{\rm s}}, \qquad (1)$$

where $\alpha$ is the BMG's thermal diffusivity, $c_v$ is its volumetric specific heat, $T_{\rm env}$ is initial temperature, $\tau_{\rm glue} \approx 0.01E$, and $c_{\rm s} = \sqrt{\mu/\rho}$ is the shear wave speed. For Zr-based BMGs, eq. (1) predicts $l_{\rm inc} \sim 10\,{\rm nm}$, below which mature shear banding cannot happen.[5)]

## 3. Molecular Dynamics Calculations

We model four metallic glasses with molecular dynamics: a binary Lennard-Jones (LJ) system, two binary embedded atom method (EAM) systems, and a quinternary EAM system. The samples were prepared by the melt-quench procedure, and deformed by supercell tilting (PBC) and moving grip (non-PBC) methods. $\tau_{\rm glue}$ values were calculated by small-scale MD simulations, and shear banding is directly observed in large-scale MD simulations.

### 3.1 Calculation of glue traction

A binary LJ $A_{80}B_{20}$ glass,[10)] and binary $Cu_{40}Ag_{60}$[11)] and $Cu_{46}Zr_{54}$[12)] glasses by EAM potentials were well characterized in the original papers, and we simply followed the same sample preparation scheme. For quinternary $Zr_{52.5}Cu_{17.9}Ni_{14.6}Al_{10}Ti_5$ system, we adopted the second-moment potential (TB-SMA) of Cleri and Rosato[13)] and took algebraic or geometric means for the cross-interaction parameters. The glass structures were generated using the melt-quench procedure starting from an fcc structure with five species of atoms randomly assigned (Fig. 1(a)). However, when quenched from above the melting temperature, the original Cleri-Rosato potential resulted in glass-glass phase separation, ZrTiAl with CuNi, shown in Fig. 1(b). To fix this problem, we tuned the potential by using newer parameters for Ni and Ti by Lai *et al.*[14)] and enhancing an attractive cross interaction uniformly by a single factor $\lambda$,

$$E_{\rm c} = \sum_i \left[ \frac{1}{2} \sum_{j \neq i} A_{\alpha\beta} e^{-p_{\alpha\beta}(r_{ij}/r_0^{\alpha\beta} - 1)} - \left\{ \sum_{j \neq i} (\lambda_{\alpha\beta}\xi_{\alpha\beta})^2 e^{-2q_{\alpha\beta}(r_{ij}/r_0^{\alpha\beta} - 1)} \right\}^{1/2} \right],$$
$$\lambda_{\alpha\beta} = \begin{cases} 1 & \text{for } \alpha = \beta \\ \lambda & \text{for } \alpha \neq \beta \end{cases}, \qquad (2)$$

where $\alpha$ and $\beta$ indicate atomic species, and $r_{ij}$ is the distance between atoms $i$ and $j$. We found the system is fully miscible when $\lambda \geq 1.3$ (Fig. 1(c)). Table 1 shows the density ($\rho$), shear modulus ($\mu$), and bulk modulus ($B$) obtained at $T = 300\,{\rm K}$ for different $\lambda$'s. We confirm that any $\lambda \geq 1.3$ can be used to demonstrate the shear band model. Here we chose $\lambda = 1.6$ as a compromise between better fitting of $\rho$ and $\mu$ to the actual material.

We generated three quinternary BMG configurations of four thousand atoms each by the procedures illustrated in Fig. 2(a). In Fig. 2(b), the responses of the glass to shear by supercell tilting method at constant strain rate $\dot{\gamma} = 10^9\,{\rm s}^{-1}$ are shown. Here, the shear stress $\tau$ is normalized by $E/2$, where $E = 71\,{\rm GPa}$ is the numerically calculated Young's modulus and 2 is the ideal Schmid factor. The maximum of these curves gives the homogeneous nucleation or rejuvenation stress $\tau_{\rm r}$, which is a property of well-aged glass. The value depends sensitively on the conditions by which the glass was made; we read $2\tau_{\rm r}/E$ to be $\sim$3.6%, 4.9% and 5.1% for the systems of case I, II, and III, respectively. In addition, $\tau_{\rm r}$ also depends on the rate of shearing[16)] as seen in Fig. 3 (where $2\tau_{\rm r}/E \sim 4.6\%$ for case III configuration with ten thousand atoms deformed at $\dot{\gamma} = 5 \times 10^9\,{\rm s}^{-1}$). In contrast, we can see the convergence of $\tau_{\rm glue}$, which is the plateau value of the stress response at large $\gamma$, for the quinternary EAM system.

Despite vast differences in the structures and interatomic interactions, the $\tau_{\rm glue}$ values obtained from small-scale MD calculations of the shear cohesive zone for the four metallic glass systems give $\epsilon_{\rm y}$ predictions in the range of 2.1%–2.9%,[5)] in fair agreement with experiments. Furthermore, these $\tau_{\rm glue}$ values are insensitive to the initial glass configuration: even the inherent structure of a high-temperature liquid,[17)] which is definitely not a glass, gives the same $\tau_{\rm glue}$ value.

### 3.2 Observation of shear band

The incubation length $l_{\rm inc} \sim 10\,{\rm nm}$ predicted from eq. (1) falls into the reach of direct MD simulations. We have performed large-scale parallel MD simulations and visualization[18)] in a thin-slab geometry to verify the ARGL model and the "march-to-melting" scenario of shear banding.[5)]

To quantify plastic deformation at the atomic level, we introduce the atomic local shear strain $\eta_i^{\rm Mises}$ for each atom $i$. Calculation of $\eta_i^{\rm Mises}$ requires two atomic configurations, one current, and one reference. First, we seek a local transformation matrix $\boldsymbol{J}_i$, that best maps

$$\{\boldsymbol{d}_{ji}^0\} \rightarrow \{\boldsymbol{d}_{ji}\}, \quad \forall j \in N_i^0, \qquad (3)$$

where $\boldsymbol{d}$'s are vector separations (row vectors) between atom $j$ and $i$ (superscript 0 means the reference configuration). Here, $j$ is one of atom $i$'s nearest neighbors, and $N_i^0$ is the total

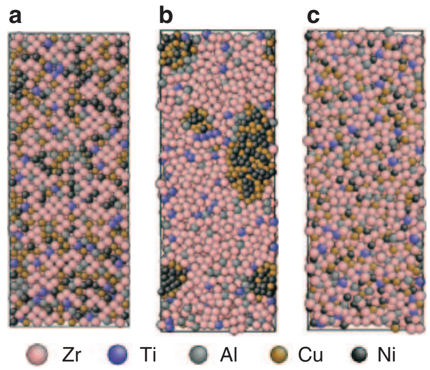


Fig. 1 Atomic configuration of $Zr_{52.5}Cu_{17.9}Ni_{14.6}Al_{10}Ti_5$ model system; (a) before melting, (b) without cross-interaction enhancement ($\lambda = 1$), and (c) with $\lambda = 1.6$.

Table 1 Properties of $Zr_{52.5}Cu_{17.9}Ni_{14.6}Al_{10}Ti_5$ model glass

| $\lambda$ | $\rho$ (g/cm$^3$) | $\mu$ (GPa) | $B$ (GPa) |
|---|---|---|---|
| 1.3 | 6.56 | 16 | 120 |
| 1.4 | 6.71 | 16 | 130 |
| 1.5 | 6.87 | 21 | 130 |
| 1.6 | 7.03 | 27 | 150 |
| 1.7 | 7.19 | 29 | 150 |
| experimental values[15] | 6.73 | 32.3 | 114.1 |

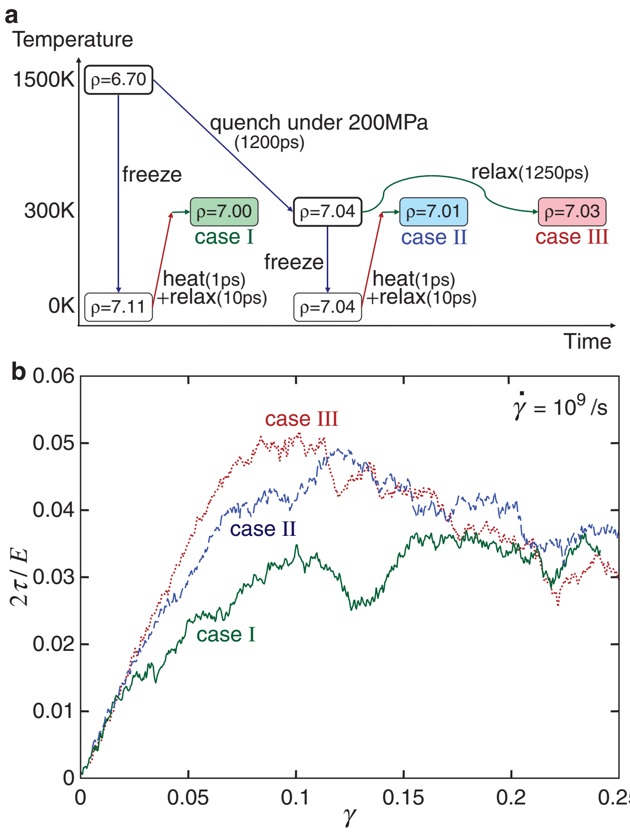


Fig. 2 (a) Preparation of three configurations for $Zr_{52.5}Cu_{17.9}Ni_{14.6}Al_{10}Ti_5$ model glass. Numbers in the boxes are density (g/cm$^3$). (b) Stress-strain curves of four thousand atom systems (4.1 nm × 4.1 nm × 4.1 nm) deformed by supercell tilting method with $\dot{\gamma} = 10^9\,\mathrm{s}^{-1}$.

number of nearest neighbors of atom $i$, at the reference configuration. $\boldsymbol{J}_i$ is determined by minimizing[19]

$$\sum_{j \in N_i^0} |\boldsymbol{d}_{ji}^0 \boldsymbol{J}_i - \boldsymbol{d}_{ji}|^2 \to \boldsymbol{J}_i = \left( \sum_{j \in N_i^0} \boldsymbol{d}_{ji}^{0T} \boldsymbol{d}_{ji}^0 \right)^{-1} \left( \sum_{j \in N_i^0} \boldsymbol{d}_{ji}^{0T} \boldsymbol{d}_{ji} \right). \quad (4)$$

For each $\boldsymbol{J}_i$, the local Lagrangian strain matrix is computed as

$$\boldsymbol{\eta}_i = \frac{1}{2}(\boldsymbol{J}_i \boldsymbol{J}_i^T - \boldsymbol{I}). \quad (5)$$

We can then compute atom $i$'s local shear invariant as

$$\eta_i^{\mathrm{Mises}} = \sqrt{\eta_{yz}^2 + \eta_{xz}^2 + \eta_{xy}^2 + \frac{(\eta_{yy} - \eta_{zz})^2 + (\eta_{xx} - \eta_{zz})^2 + (\eta_{xx} - \eta_{yy})^2}{6}}. \quad (6)$$

Like Falk and Langer's $D_{\mathrm{min}}^2$,[19] $\eta_i^{\mathrm{Mises}}$ is a good measure of local inelastic deformation. This measure has been incorporated into our visualization program AtomEye.[20]

In Fig. 3, atoms are colored by $\eta_i^{\mathrm{Mises}}$ calculated with $\Delta\gamma = 0.01$ between the current and reference configurations. Before the shear stress reaches maximum, no significant local deformation is seen (inset image a). At $\gamma = 0.1$, small stress drops can be seen in the stress-strain curve and correspondingly we see some shear transformation zones (STZs) in snapshot (b). We see STZs coalesce to become ESB when the shear stress drops in cascading fashion at $\gamma = 0.14$ (c), and then this ESB diffuses out at $\gamma = 0.18$ (d). The same process then recurs a few times with increasing $\gamma$.

Large-scale MD simulations of the binary LJ system with 5 million atoms were then performed. The system was prepared identically as that of Varnik *et al.*,[10] but with a much larger dimension of $800b \times 400b \times 16b$ as illustrated in Fig. 4(a). The thickness in $z$ is intentionally chosen to be small so we can reach the incubation sizescale (and exceeding the thermal diffusion lengthscale $\sqrt{\alpha t}$) in $x$ and $y$. Here, we use the mean atomic spacing $b \equiv \rho_N^{-1/3}$ as length unit and $b/c_s$ as time unit, where $\rho_N$ is the number density of atoms. In Zr-based BMG, they are estimated to be $b \sim 0.26$ nm and $b/c_s \sim 0.1$ ps.

Mode-III (anti-plane shear) loading which was applied by constant forcing on the grips to realize simple shear loading condition. Note that mode-III generates only shear stress while mode-I and II will generate compressive or tensile normal stress as well as shear stress. At each MD step, force $f_{z\pm} = \pm(A/N_\pm)\tau_{\mathrm{grip}}$ is applied to each atom in the upper/lower grip region, where $A$ is the area of grip and $N_\pm$ is the number of atoms in the grip. No thermostat was applied after equilibration. For each case of $2\tau_{\mathrm{grip}}/E = 0.021$ and 0.027, a shear band embryo was introduced at the beginning by the instantaneous displacement of atoms according to the displacement field solution of a smeared super screw dislocation. In the former case of $\tau_{\mathrm{grip}} < \tau_{\mathrm{glue}}$, the introduced

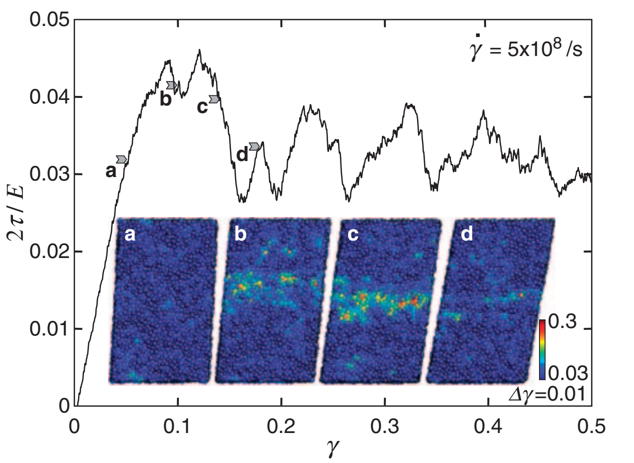


Fig. 3 Stress-strain curves of ten thousand atom system (case III: 6.4 nm × 10.8 nm × 2.5 nm) deformed by supercell tilting method with $\dot{\gamma} = 5 \times 10^8\,\text{s}^{-1}$. Inset images are snapshots of atomic configuration at $\gamma = 0.05$ (a), 0.1 (b), 0.14 (c), and 0.18 (d). Atoms are colored according to their atomic shear strain $\eta_i^{\text{Mises}}$.

embryo (Fig. 4(b)) does not propagate, becomes diffuse, and eventually dies (Fig. 4(c)). In the latter case of $\tau_{\text{grip}} > \tau_{\text{glue}}$, the introduced embryo started to develop into MSB. Near the tip of ESB, it is observed that STZs coalesce and the width of the ESB has grown up to $\sim 75b$ (Fig. 4(d)). The local temperature of the system is monitored simultaneously. It is seen that, at $t = 7800b/c_s$ (Fig. 4(f)), the local temperature at the center of the shear band has reached $T_g = 0.435$, signifying the ESB has indeed matured, becoming a bona fide shear crack, since the newly formed $T > T_g$ zone has much lower viscosity and can be regarded as traction free. Movies of the evolution of shear strain and temperature in this simulation can be viewed at.[18]

We also performed another control calculation, where $2\tau_{\text{grip}}/E = 0.03$ was applied but no embryo was introduced at the beginning. In this case, nothing happened within the MD simulation timeframe ($t = 4000b/c_s$). This should be expected since $2\tau_{\text{grip}}/E < 2\tau_r/E \simeq 0.05$, the homogeneous nucleation stress.

## 4. Conclusion

In the ARGL shear band model, it is argued that the far-field shear stress, $\tau_\infty$, must exceed the quasi steady-state glue traction, $\tau_{\text{glue}}$, for an embryonic shear band to propagate. $\tau_{\text{glue}}$ values were calculated by small-scale MD simulations of the shear cohesive zone and it is shown that $\tau_{\text{glue}}$ values are insensitive to the initial glass configuration. The results of large-scale MD simulations are summarized as that shear banding requires (a) an embryo with long aspect ratio, (b) $\tau_{\text{grip}} > \tau_{\text{glue}}$, and (c) the size of $\tau_{\text{grip}} > \tau_{\text{glue}}$ region must exceed $l_{\text{inc}} \sim 10\,\text{nm}$ in eq. (1). When (a), (b), (c) are satisfied, we will see mature shear bands form with eventual liquid or near-liquid tails, dramatic softening and load shedding. If any of (a), (b), (c) conditions are not satisfied, there will be no sharp local temperature rise,[21] and even if a shear band is introduced it will smear out.

MD contributes to this theory of shear banding by

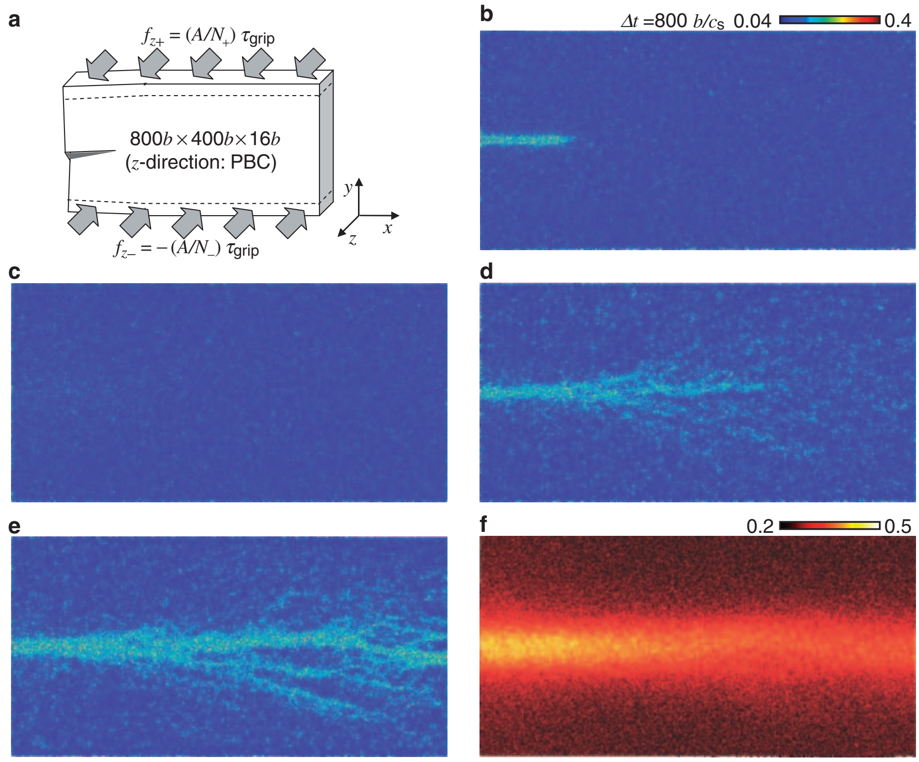


Fig. 4 (a) Molecular dynamics simulations of a binary LJ system with 5 million atoms. Atomic configuration snapshots for (b) $2\tau_{\text{grip}}/E = 0.021$ at $t = 1000\,b/c_s$ and (c) $2500\,b/c_s$; (d) for $2\tau_{\text{grip}}/E = 0.027$ at $t = 2500\,b/c_s$ and (e) $4000\,b/c_s$. Atoms in (b–e) are colored according to their atomic shear strain $\eta_i^{\text{Mises}}$. (f) Temperature distribution ($T_g = 0.435$) for $2\tau_{\text{grip}}/E = 0.027$ at $t = 7800\,b/c_s$. Melting, predicted in,[5] indeed occurs within a simulation run length ~100 nm.

providing decent values for $\tau_{glue}$ and therefore $\epsilon_y$ compared to experiments, and elucidating its microscopic origin.[5] It turns out $\tau_{glue}$ is not an intrinsic property of well-aged glass, but that of a strongly driven, non-equilibrium material - the cold "glue" state inside shear cohesive zone - which only exists transiently, but nonetheless controls the macroscopic $\epsilon_y$ of BMG. $\tau_{glue}$ reflects the effect of alienation (disruption of atomic short-range order, including chemical order), and its steepest-descent-like recovery on the energy landscape, occurring at picoseconds timescales. The significant flattening of the amorphous-amorphous shear cohesive law (aka generalized stacking fault energy)[5] can be well-explained by this disruption of chemical order[6] ("chemical softening"), without the need of thermal softening. Catastrophic thermal softening does eventually arise, however, if an embryo runs in a critical sized volume ($l > l_{inc}$) with a critical stored elastic strain-energy density ($\tau > \tau_{glue}$), as shown in our simulation.

## REFERENCES


1) W. L. Johnson: J. Miner. Metall. Mater. Soc. **54** (2002) 40.
2) W. L. Johnson: Invited talk at bulk metallic glasses IV conference, (Gatlinburg, TN, 2005).
3) E. Pekarskaya, C. P. Kim and W. L. Johnson: J. Mater. Res. **16** (2001) 2513.
4) B. Yang, M. L. Morrison, P. K. Liaw, R. A. Buchanan, G. Y. Wang, C. T. Liu and M. Denda: Appl. Phys. Lett. **86** (2005) 141904.
5) F. Shimizu, S. Ogata and J. Li: Acta Mater. **54** (2006) 4293.
6) D. B. Miracle: Nat. Mater. **3** (2004) 697.
7) V. Viasnoff and F. Lequeux: Phys. Rev. Lett. **89** (2002) 065701.
8) M. Ortiz and A. Pandolfi: Int. J. Numer. Methods Eng. **44** (1999) 1267.
9) S. Ogata, J. Li and S. Yip: Science **298** (2002) 807.
10) F. Varnik, L. Bocquet and J. L. Barrat: J. Chem. Phys. **120** (2004) 2788.
11) Y. Qi, T. Cagin, Y. Kimura and W. A. Goddard: Phys. Rev. B **59** (1999) 3527.
12) G. Duan, D. H. Xu, Q. Zhang, G. Y. Zhang, T. Cagin, W. L. Johnson and W. A. Goddard: Phys. Rev. B **71** (2005) 224208.
13) F. Cleri and V. Rosato: Phys. Rev. B **48** (1993) 22.
14) W. S. Lai, Q. Zhang, B. X. Liu and E. Ma: J. Phys. Soc. Jpn. **69** (2000) 2923.
15) Z. Bian, M. X. Pan, Y. Zhang and W. H. Wang: Appl. Phys. Lett. **81** (2002) 4739.
16) S. Ogata, F. Shimizu, J. Li, M. Wakeda M and Y. Shibutani: Intermetallics **14** (2006) 1033.
17) F. H. Stillinger and T. A. Weber: Phys. Rev. A **25** (1982) 978.
18) http://alum.mit.edu/www/liju99/Papers/07/Shimizu07/
19) M. L. Falk and J. S. Langer: Phys. Rev. E **57** (1998) 7192.
20) J. Li: Model. Simul. Mater. Sci. Eng. **11** (2003) 173.
21) J. J. Lewandowski and A. L. Greer: Nat. Mater. **5** (2006) 15.